MULTI-STORIED LANDSLIDES AND STRENGTH OF SOFT CLAYS
GLISSEMENT DE TERRE A PLUSIEURS ETAGES ET LA RESISTANCE DES ARGILES TENDREES

G. I. TER-STEPANIAN, Dr. Sc. Prof.
Armenian Academy of Sciences, Yerevan, Armenia, USSR.

M.N. GOLDSTEIN, Dr. Sc. Prof.
Railway Institute, Dnepropetrovsk, USSR.

SUMMARY. I. Sliding of some slopes proceeds in several stories located one above another; these movements may be of different type and go on along divergent trajectories with dissimilar rates. The resolution of vectors of rates of displacement of surface benchmarks and the determination of outlines of different stories of sliding may be made graphically, taking into account the type and distribution of landslide fissures, deformation of constructions and geological conditions.

2. The experiments have shown that the residual shear strength is almost the same for clays of different type and origin and coincides well with the average shear strength calculated from the slide data along the actual surfaces of sliding. The gradual alteration of clay particles orientation proceeds by deformation of soil. The shear diagram in terms of octahedral effective stresses is the same for different test conditions and initial state of clays.

The paper contains some results of investigations of landslide phenomena performed in recent years in Yerevan and Dnepropetrovsk. The first part of the paper is written by Prof. Ter-Stepanian and the second-by Prof. Goldstein with collaborators.

I. On Mechanism of Multi-Storied Landslides.

a) Conditions of formation of multi-storied landslides

Slopes are subdivided into simple and complex ones. Simple slopes are formed by two horizontal planes connected by one inclined plane. Short and long slopes may be distinguished among simple slopes; this subdivision does not imply the absolute length of slopes but rather the relation between this length and the thickness of loose rocks.

Short simple slopes are composed of rheologically homogeneous soils; the height H of such slopes is comparable with depth h of earth masses involved in sliding (Fig. I, a). High natural slopes composed of homogeneous soils belong to this category too if they have plane inclined surfaces.

In the majority of simple short slopes zones C of rotational depth creep is located in the middle and lower parts of the potential surfaces S of sliding. In these zones values of the coefficient tan θ of mobilized shear strength exceed the limiting values tan θ_0 corresponding to the shearing resistance τ_0 .

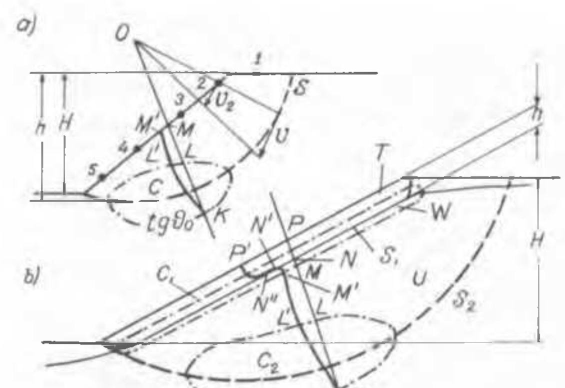

Fig. I. Simple slopes: a) short slope; b) long slope.

An orbitrary radial straight line KM is shown on Fig. I, a; after deformation it takes the shape KM'. Here the contortion due to depth creep takes place on the portion KL' and rigid displacement on the portion L'M.

Such a picture takes place in the initial phase of depth creep when the influence of deformation on stress distribution in massif is negligibly small. The redistribution of tangential stresses occurs further and the zone of rotational depth creep stretches along the potential surface of sliding.

If the potential surface of sliding touches competent rocks, zone of secular depth creep may originate in rocks adjacent to the contact (Ter-Stepanian, 1968); low values of the gradient of strain rate is characteristic for this zone.

If should be emphasized that there is only one potential circular surface of sliding and only one zone of rotational depth creep, attached to this surface. Long-term shear strains proceed in this zone in the phase preceding the failure.

Long- simple slopes are characterized by plane potential surfaces of sliding S which are parallel to the slopes (Fig. I,b); their position is determined by geological features (planes of bedding, of tectonic fissures, the contact of products of weathering with rocks etc.). The case when talus deposits T are lying over the inclined surface of bedrocks U is shown on Fig. I, b.

Usually the height H of such slopes essentially exceeds the thickness h of the sliding earth masses; this enables to use the simplifying concept of an infinitely long slope (Taylor, 1948). Zone C_1 of planar (translational) depth creep is attached to the mentioned potential plane of sliding S_1.

Secular depth creep is developed in the slope body located beneath the potential plane of sliding and composed of bedrocks. If the bedrock strata dip steeply into the slope or are vertical, slow outcrop curvature is developed in weathered bedrocks W.

Considering a long simple slope in whole, one can notice the potential circular surface of sliding S_2 too; by deterioration of static conditions the failure of the slope is most probable along this surface. Deeply located zone C_2 of rotational depth creep is attached to this surface of sliding.

The character of deformation in this zone is shown on Fig. I,b. The orbitrary radial straight line KP after deformation takes shape KP'. Here S-like secular creeping of strata takes place in the portion KL'; the rigid displacement of bedrocks U due to this creeping of underlying rocks in the portion L'M'; secular terminal creeping of covered strata in weathered bedrocks W - in the portion M'N', and finally, the planar depth creep of talus deposits T - in the portion N'' P' (Ter-Stepanian 1966, b). The gap N'N" of the deformed line is observed on the contact of talus deposits with underlying weathered bedrocks W due to the difference of deformative properties of these rocks.

It should be emphasized that two potential surfaces of sliding exist in long simple slopes and two zones of depth creep are attached to them, a planar zone in the upper part of the slope and a rotational one in the depth. The existence of these two zones does not indicate the abnormality in distribution of shear stresses but demonstrates that there are two areas in the slope body where the relation between values of the coefficient tan θ of mobilized shear strength and the limiting values of this coefficient tan θ_0 for the corresponding rocks satisfies the condition of depth creep ($\tan \theta > \tan \theta_0$).

These zones of depth creep are stretched along the potential surfaces of sliding due to the redistribution of shear stresses in the process of creeping.

The depth creep of short simple slopes (Fig. I, a), if they are not high and of the subsurface parts of high long simple slopes (Fig. I, b, zone C_1) is of periodical nature; its rate is determined by the intensity of slide-producing agents. It is connected with the permanently acting causes, on which seasonal phenomena are superposed (fluctuation of pore pressure, of weight by wetting etc.).

In distinction to this the depth creep of short simple slopes (Fig. I,a), if they are high, and of the deep parts of high long simple slopes (Fig. I, b, zone C_2) may be of secular nature; its rate is essentially low and is determined by permanently acting agents (retreat of the sea, change of inclination of the surface due to tectonic uplift etc.).

Slopes are complex if they are formed by intersection of several, differently inclined planes or curvilinear surfaces (Fig. 2)

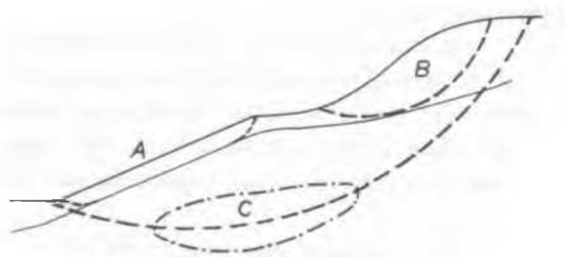

Fig. 2. Complex slope.

Geologically they may be composed of different dense and loose rocks with diverse type of bedding. The majority of natural high slopes belongs to this group. Small slants ') with simpler shapes are easily distinguished on the surface of such slopes. Such slants or slopes of second order are connected by transitional lots having small inclination. Separately taken, each slant is characterized by a definite distribution of tangential stresses in its body and therefore potential surfaces of sliding and attached to them zones of depth creep may be separated. Depending on the geological structure and sizes planar A and rotational B zones of depth creep may develop in slants. The experience shows that indeed separate landslides render more active on complex slopes, the depth creep increases, the phase of failure developes etc. Thus such lots of complex slopes behave as separately taken simple slopes. Some of them may deform slowly and constantly while others - quickly and jumplike depending on the mechanism of each of these small slidings.

However, taken in whole, the body of a high complex slope is characterized also by a

') Here small elements of complex slopes are called slants, the term being somewhat conditional.

special stress state as it is the case with a simple short slope, which it generally resembles. In such high slopes potential surface of sliding exists in depth, and an attached zone of rotational depth creep C which may be of secular nature. The regime of this deformation may differ essentially from that of deformation which proceed in upper stories, since they are produced by dissimilar factors.

Instrumental measurements of the displacement of rocks on such slopes reveal a complicated picture, caused by superposition of displacements in different zones of depth creep, with dissimilar regimes of deformation. Its interpretation is impossible unless a true notion of the mechanism of sliding of such a complex slope, the location and significance of different zones of depth creep is formed.

b) Methods of Analysis of Complex Sliding of a Slope.

Usually the picture of sliding of high-natural slopes in apace and time is very complicated, and as a matter of fact we are only approaching the formulation of this problem. Simpler and more available for analysis is the case when the landslide-producing factors act on the slope with a constant intensity for a long time. Thus conditions of steady sliding are gradually created.

Steady sliding assumes the invariability of all parameters which characterize the process: the distribution of stresses in the slope body, the deformative properties of soils, the distribution of values of the coefficient of mobilized shear strength, the contours of the depth creep zone, the distribution of displacement rates etc. Such an analysis fails since it assumes the constant rate of displacement during the years, the assumption being evidently not always valid. The assumption of steady sliding may be just for deeply located zones of secular depth creep; it must be used with care in reference to superficial zones of creep.

The regime of unsteady creep is specific for the superficial zones, all parameters being changed in time, However, due to the intricacy and unsufficient scruting of the problem only a qualitative estimation may be made at present regarding unsteady creep.

The case of steady creep is considered in the present work. As an approximation to this case average rates of displacement are commonly used. They are calculated from results of observation of slope deformation made during many years. Even at this simplified approach usually a rather involved picture is revealed.

In many cases the map of vectors of displacement (or rates of displacement) shows great divergence of the magnitude and direction which permits to get only a general idea on sliding. If there is no doubt on the exactness of geodetic measurements one of the probable causes is apt to be the superposition of several simple slidings, executed in different stories. The aim of analysis is the resolution of displacement rate vectors into components relating to different stories of sliding.

Results of geodetic measurements are usually given as values of increments of coordinates Δx, Δy and Δz, corresponding to the time interval Δt. Then components of displacement rate vector v may be computed

$$v_x = \frac{\Delta x}{\Delta t}, \quad v_y = \frac{\Delta y}{\Delta t} \quad \text{and} \quad v_z = \frac{\Delta z}{\Delta t}$$

and the magnitude of the horizontal projection v_h of the displacement rate vector

$$v_h = \sqrt{v_x^2 + v_y^2}$$

Two diagrams are drawn, one showing the horizontal plane (with coordinate axes v_x and v_y, Fig. 3, a) and the other - the vertical plane passing through the total displacement rate vector v (with coordinate axes v_h and v_z, Fig. 3, b and c). These diagrams may be considered as hodographs of the displacement rates of sliding assuming that the process is continuous.

The resolution of displacement rate vectors is made graphically on the above-mentioned drawings. Let us consider several schemes of sliding and corresponding hodographs; let five benchmarks are placed on the slope numbered from I to 5, counting downslopes (Fig. I, a).

I. A plane slope dips to the north. Planar depth creep takes place on the slope, the motion being uniform. In this case the ends of displacement rate vectors are located in a small area A (Figs. 3, a and b). The vector for the benchmark No. 3 is shown on the diagrams. The scattering of points in limits of area A is explained by arrors of observation.

2. Plane slope dips to the north-east. Planar depth creep develops on the slope. The seat of sliding is located in the upper part of the slope and therefore the sliding is of an advancing type. The ends of vectors are located in a narrow stretched area B (Figs. 3, a and b).

3. Plane slope dips to the east. The seat of sliding is located in the lower part of the slope the sliding being of a retreating type. The ends of vectors are located in the area C (Figs. 3, a and b).

4. Plane slope dips to the south-east. The sliding seat is located near the benchmark No. 2. In the area which is located upslopes from this benchmark, the retreating slide takes place while in the downslope area the advancing one. Such a case is shown on the diagrams by the area D (Figs. 3 a and b).

5. There is no displacement of benchmarks on the slope. Such a case corresponds to the area E (Figs. 3 a and b).

6. The slope dips to the north-west. Rotational depth creep develops in soft clays composing the slope body. The rate v of all points of the potential surface is constant (Fig. I, a). The rate v_i of all surface benchmarks is obtained from a simple geometrical relationship; the construction for the benchmark No. 2 is made on Fig. I, a. Ends of displacement rate vectors are located in area F (Figs. 3 a and c).

7. The same case as the previous one; the sliding seat is located in the upper part

of the slope and the displacement is of advancing type. Ends of rate vectors are in the area G (Figs. 3, a and c).

8. The slope dips to the south. Slow earthflow proceeds on the slope. Due to features of the relief the earthflow forms a smooth arc in plane, the concavity being turned towards the east. The sliding is uniform. Such a case is shown on diagrams by area H (Figs. 3 a and c).

9. The same case as the previous one, but the sliding seat is located in the lower part of the slope and the process of retreating type. Ends of rate vectors are in the area K (Figs. 3, a and c).

depth creep of the first story (i. e. of the whole slope) and the vector v_N illustrating the creep of the second story (i. e. of the slow earthflow properly). The resolution of the displacement rate vector for the benchmark No. 4 is shown on Figs. 3, a and c.

Thus the deformation of the slope as a whole is represented by the area M; the relative creep rate of the earthflow is illustrated by vectors v_N, having their beginnings in the area M and ends in the area N.

The position of the area M is determined by location of points 6, 7 ..., corresponding to benchmarks placed on the slope outside of the earthflow.

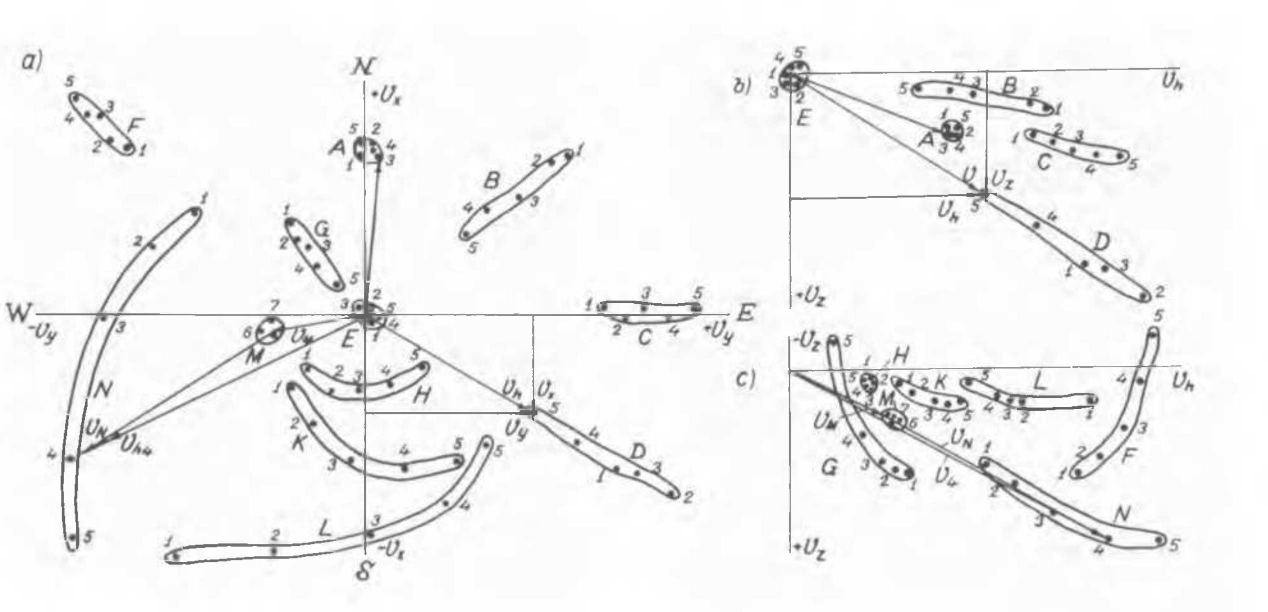

Fig. 3. Hodographs of sliding; a) horizontal plane, b) and c) vertical planes.

10. The same case as two previous ones, but the sliding seat is located in the upper part of the slope and the process is of advancing type. Ends of rate vectors are in the area L (Figs. 3, a and c).

11. The slope dips to the west; it deforms slowly as a whole. Planar depth creep in the first story has secular nature. A slow earthflow proceeds in the second story, as it is described in point 8. The earthflow is directed in the upper part of the slope to the north-west, in the middle part-to the west and in the lower part-to the south-east; thus the earthflow forms an arc with concavity turned towards the south. Such a case is presented by the area N (Figs. 3, a and c).

Horizontal projection of displacement rate vectors v_h for benchmarks placed on the slow earthflow have their beginning in the origin O of coordinates and ends in points 1, 2 ... 5 of the area N. Each of these vectors may be graphically resolved into two vectors: the vector v_M which characterizes the

It stands to reason that the described schemes do not exhaust all possible types of sliding. Other types of slope deformation may be added to them based on the same principle of analysis.

Using this method one can easily analyze the sliding of slopes by applying in principle the same procedure which serves for the resolution of a complex oscillating movement into a series of harmonic oscillations.

c) Practical Application of the Method

The analysis of the landslide mechanism begins from the preparation of two described diagrams (Fig. 3). Points refering to the separate sliding bodies are located on these diargams either assembled in groups (in the sliding is uniform) or stretched if strips (if the sliding is progressive, i. e. is of advancing or of retreating type). Corresponding types of sliding and mechanisms of landslides are shown above.

Recognition of stories of sliding must be made in course of joint analysis of the geological and geohydrological conditions of the slope, geomorphological features and the history of development of the relief (Terzaghi I950; Skempton, I964; Bjerrum, I967).

Outlining of separate stories of sliding as they are reflected on the surface is promoted essentially if the landslide fissures and the deformation of structures are taken into account. It was shown previously that the type and location of fissures are closely connected with the distribution of stresses in the sliding body (Ter-Stepanian, I962).

The use of landslide fissures fails sometimes since these fissures may be closed with the time due to the surface creep (solifluction), or they can not even develop in the thin superficial sheet, although the discontinuity may exist in the subsoil.

From this point of view in some cases structures located on the slope give much information about the deformation of the supporting soil. Particularly useful for analysis of landslide dynamics are deformed concrete ditches, stone and concrete borders of roads, light brick houses etc. A map showing all such deformation of landslide origin is of invaluable importance for the analysis of sliding.

Fig. 4 may serve as an illustration of possibilities given by the described method; it shows a landslide in Sochi, on the Caucasian coast of the Black Sea. Three stories of sliding were detected on this slope; their boundaries are marked by figures I to 3.

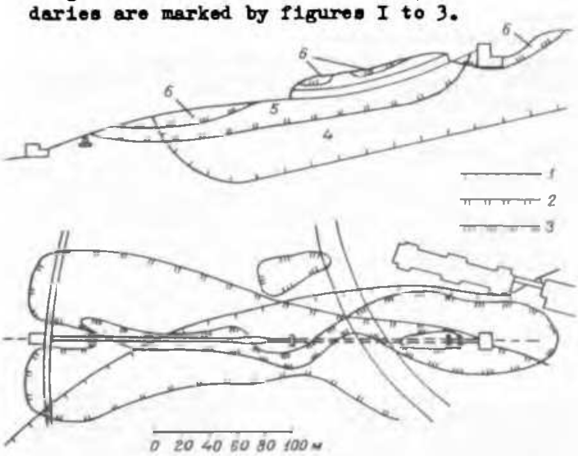

Fig. 4. Three-storied landslide in Sochi.

The first story is a rotational sliding; it envelopes blocks of argillites and sandstones 4 with a depth up to 60 metres. The second story is a planar sliding; crushed argillites 5 with a thickness up to 20 metres are involved in motion. The third story is a slow earthflow 6 which develops in the colluvial cover up to 6 metres thick. All these slidings are in the phase of depth creep. More detailed description of this instructive landslide is given in other publications (Ter-Stepanian, I966 a, I967).

Another big two-storied landslide is taking place in Armenia near the medieval temple of Geghart. Here a huge rock slide is formed due to the deep cutting of the river Azat. Two earthflows pass along the contact line of this landslide with the immovable massif.

Obviously multi-stories landslides are not unusual phenomena, especially in young highlands, on sea coasts and on the banks of rejuvenated rivers. Their mechanism is determined by the geological structure of slopes, their geometric characteristics and the history of sliding.

Using the graphical resolution of displacement rate vectors into components, related to different stories of sliding, the involved picture of slope dynamics may be interpreted and the mechanism of sliding revealed.

2. On Strength of Soft Clays.

The model studies of the stability of clay slopes were carried out by the big centrifugal apparatus described elsewhere (Goldstein et al., I96I).

Deformation of a clay having stiff consistency appeared at first in the lower part of the slope when the height of the slope was 7,5 m (the slope angle 45°). The upper part of the slope underwent some settlement.

The deformation increased gradually with the height of the slope. The region of a plastic flow with a marked thin zone of the intensive shear in it began to spread up in the slope.

The slope settled a little more and became more gentle; the tension cracks appeared behind the upper edge of the slope. The deformation of the slope was accompanied with the bulge of the base.

When the stress state of the slope reached the critical point, a sudden failure occured. The lower part of the slope moved at first; it was followed by the upper one (Fig.5).

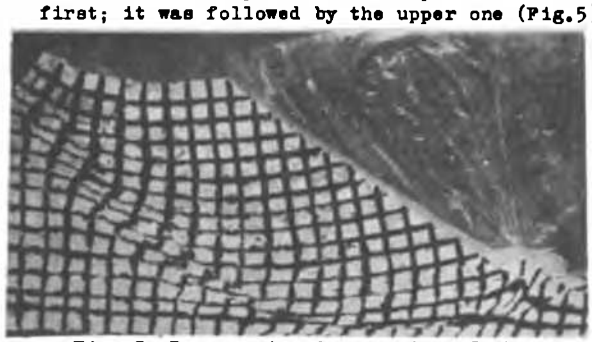

Fig. 5. Progressive destruction of the slope model.

These tests show distinctly that the plastic flow in a slope begins as a local phenomenon. In separate points the shear strength becomes less then the shear stress.

The original bonds between the soil particles are gradually destroyed. Reorientation of clay particles proceeds followed by the strength reduction. Then the stress redistribution takes place leading to the further reduction of soil strength and to the stress concentration in the more rigid points.

If these stresses exceed the longterm strength of the soil in these points the plastic flow spreads out more and more; this process is ended by the brittle rupture of the slope as a whole.

The quantitative reduction of the strength was invertigated in the model tests by cutting off the slide tongue after every slide cycle completion.

The corresponding shear strength s_r was calculated proceeding from factor of safety equal to one. The shear strength of the clays was investigated also by means of ring-shear apparatus with authomatic record device.

The reduction of the shear strength from the peak values s_f to the lower s_r value (Goldstein, 1964; Skempton, 1964) took place only in the clayey soils, whereas in the sandy and silty seams the strength reduction during the deformation was absent (Goldstein et al., 1968).

The shear rate decrease in 1000 times results the reduction of peak strength in 1,5 - 2 times; under the various normal pressure the peak strength remains practically the same.

So the peak shear strength is due mainly to the interparticle forces which is little affected by external pressure. On the contrary the residual strength is proportional to the normal stress on the shear surface, but it is independent on the rate of shear. It is very interesting to note that s_r under the same normal pressure is almost the same for different clayey soils with very different peak strength (from decimals up to 5 kg/cm^2).

The following dependence was found from more than 200 shear tests

$$s_r = 0{,}09 + 0{,}14\,\sigma \qquad (1)$$

with the correlation factor 0,78.

The investigation of the natural sliding slopes has shown that the decrease of strength of the soil to the residual values almost equal to the laboratory values s_r proceeds also in the zone of displacement (Turovskay et al., 1964).

For more than 50 actual landslides in plastic clays the mean shear strength s_f on the slide surfaces is equal to

$$s_f = 0{,}06 + 0{,}15\,\sigma \qquad (2)$$

where σ - the mean normal stress on the slip surfaces; the correlation factor equals to 0,82.

The parameters of these two equations are very close to each other.

The connection between the clay strength and the microstucture of clay was also investigated. Orientation of clay particles was investigated by means of polarizing microscope¹) The microstructure was studied after the triaxial shear test, after the ring shear test, and in samples obtained from the actual landslides.

The particles arrangement was presented by the circle diagram (Fig. 6).

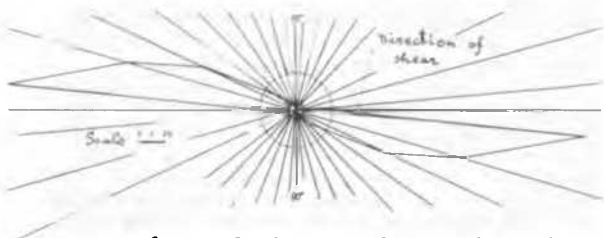

Fig. 6. Circle diagram of the orientation of clay particles after ring-shear test, a - direction of shear.

The length of the radii of the diagram is proportional to the percentage of particles oriented in this direction (Turovskaya, 1957, 1964). Before the deformation the diagram is almost circular.

In the triaxial test the particle orientation becomes at first almost horizontal and normal to the σ_1 direction. When $\sigma_1 - \sigma_3$ increases the particles gradually become oriented under the acute angle to the σ_1 direction.

The sand grains admixture prevents from the clay particles orientation forming some kind of dowels and increases the residual shear strength of the soil.

The visible orientation of particles is absent at maximum shear strength in the quick ring shear tests. The clay particles along the surface of displacement are oriented good in samples reached steady shear strength. The circle diagram have been stretched along horizontal axis (Fig. 6).

The orientation had expressed poorly on some distance from zone of the maximum orientation; in our tests it was equal nearly 0,3mm But shear line is observed again on the distance about 1,5 mm from main shear zone.

The samples from main scarp are defined by almost homogeneous microstructure without visible orientation of particles.

The samples from zone of slide displacement are defined by sharply expressed orientation of the clay particles. It testifies to plastic flow of the material (Fig. 7).

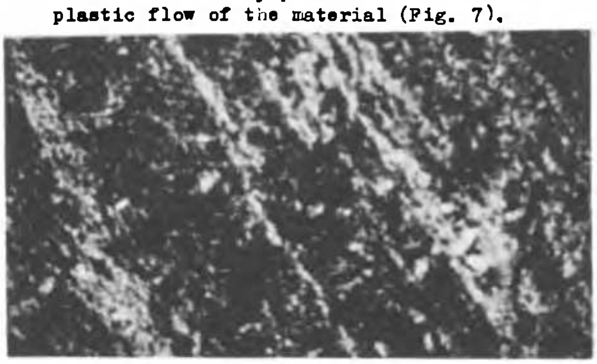

Fig. 7. Microstructure of clay from the landslide shear zone.

¹) Orientation of clay particles at shear was established by G. Ter-Stepanian (1936) using the indirect method.

The orientation results the increase of the suction potential, which causes the moisture migration and increasing of the water content in the shear zone.

It is very difficult to preserve constant the physical state of soil during the strength tests. Therefore the shear diagram is inclined usually and the parameters of the diagram depend on test conditions. These parameters are not a physical constants of the soil (Babitskay, 1965).

The tests have shown that the shear diagram in terms of octahedral effective stresses ($\bar{\sigma}_o$ versus τ_o) is the same for different test conditions (UU, CU, CD) and for different initial water content and density (Fig. 8).

The pore pressure is a very sensitive indicator of changes soil physical conditions. It can be seen from comparison of the test results when pore pressure isn't taken into consideration (Fig. 9, a) and when it is (Fig.9b)

A great scattering takes place on the diagram (σ versus τ) because the change of the physical condition was not taken into consideration.

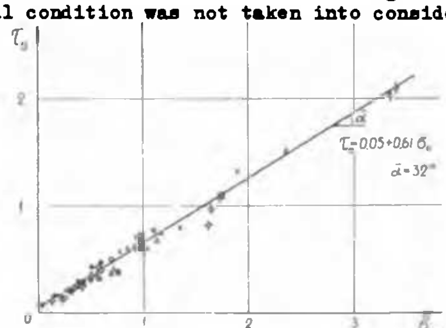

Fig. 8. Shear diagrams of clayey soil in terms of effective octahedral stresses.

The envelope of the effective Mohr's circles is quite reliable. Points on the Fig. 9,b show shear strength in terms of effective octahedral stresses $\bar{\sigma}_o$. All points are lying on the envelope of Mohr's circles. The Mohr's criterion coincides with the criterion of failure in the terms of the octahedral effective stresses. Then one may not take into consideration the intermediate stress by the investigation of clays.

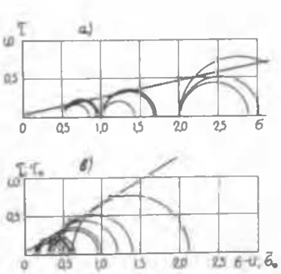

Fig. 9. Shear diagram of clayey soil in terms of total (a) and effective (b) stresses.

Conclusion.

I. Terzaghi's idea concerning the progressive failure of slopes was confirmed by centrifugal machine tests.

2. In process of long-term shear deformation the strength of different clays is reduced to more or less close values. It can be explained by orientation of clay particles when their equally charged basal surfaces coincide with the shear surface. One can observe the moisture migration to the microzone of displacement.

3. It can be recommended by calculations to assume the residual strength as the shear strength in the zone of progressive failure.

4. The shear diagram in terms of effective stress doesn't depend on test conditions.

For acceleration of tests it can be suggested to test the saturated clays in conditions of uncompleted consolidation with pore pressure measurements.

REFERENCES.

BABITSKAYA S.S. 1965. On strength of saturated clayey soil. "Questions of geotechnics", Moscow 9:32-36 (in Russian).
BJERRUM L., 1967. Progressive failure in slopes of overconsolidated plastic clay and clay shales. Journal, Soil Mech. and Found. Div., ASCE 93: SM 5:1-49; Norwegian Geotechnical Institute Publications 77:1-29.
GOLDSTEIN M.N. and Babitskaya S.S., 1964. Calculation of stability of slopes with regard to creeping shear. "Questions of geotechnics", Moscow, 7 (in Russian).
GOLDSTEIN M.N. Misumsky et al., 1961. The theory of probability and statistics in relation to the rheology of soils. Proc., Fifth Intern. Conf. Soil Mech. Found. Engg., Paris I:123-126.
GOLDSTEIN M.N., Turovskaya A.J. et al., 1968. Investigation of deep landslides of Odessa "Questions of geotechnics", Kiev, 12:7-36 (in Russian).
SKEMPTON A.W., 1964. Long term stability of clay slopes. Geotechnique, 14:2:77-101.
TAYLOR D.W. 1948. Fundamentals of soil mechanics. New York, Wiley.
TER-STEPANIAN G. 1936. On the influence of scale-like shape of clay particles on the process of shear in soils. Proc., Intern. Conf. Soil Mech. Found Engg., Cambridge, Mass. 2:112-116.
TER-STEPANIAN G. 1962. Klassifizierung der Erdrutschrisse, Geol. u. Bauwesen, 28:1:43-54.
TER-STEPANIAN G. 1966a. Discussion on Earth and Rock Dams, Slopes and Open Excavations. Proc., Sixth Intern. Conf. Soil Mech. Found. Engg., Montreal 3:283-284.
TER-STEPANIAN G., 1966b. Types of depth creep of slopes in rock masses. Proc., First Congress Intern. Soc. Rock Mech., Lisbon, 2:157-160.
TER-STEPANIAN G. 1967. The use of observations of slope deformation for analysis of mechanism of landslides. Problems of geomechanics, Yerevan 1:16-57.
TER-STEPANIAN G.1968. On secular depth creep of slopes. Problems of geomechanics, Yerevan 2:1-23.

Terzaghi K., 1950. Mechanism of Landslides. Geol. Soc., Am. Berkey vol. 83-123.

Turovskaya A.J., 1957. On the influence of deformation on the structure of clayey soils. Dnepropetrovsk (in Russian).

Turovskaya A.J., 1964. On structure of soil in the shear zone; "Questions of geotechnics", Moscow, 7 (in Russian).

Turovskaya A.J., and Pergamenshchikov A.S., 1964. Shear strength of clayey soils in the zone of landslide displacement. "Questions of geotechnics", Moscow 7 (in Russian).